

# <sup>17</sup>O NMR AND DFT STUDY OF HYDROGEN BONDING: PROTON SHARING AND INCIPIENT TRANSFER

V. Balevičius<sup>a</sup>, K. Aidas<sup>a</sup>, A. Maršalka<sup>a</sup>, F. Kuliešius<sup>a</sup>,

V. Jakubkienė<sup>b</sup>, and S. Tumkevičius<sup>b</sup>

<sup>a</sup>*Institute of Chemical Physics, Vilnius University, Saulėtekio 3, 10257 Vilnius, Lithuania*

<sup>b</sup>*Department of Organic Chemistry, Vilnius University, Naugarduko 24, 03225 Vilnius, Lithuania*

Email: vytautas.balevicius@ff.vu.lt

Received 16 June 2022; accepted 30 June 2022

<sup>17</sup>O NMR spectra of pyridine *N*-oxide (PyO) complexes with the acids – acetic (AA), cyanoacetic (CyA), propiolic (PA), trichloroacetic (TCA), trifluoroacetic (TFA), hydrochloric (HCl) and methanesulfonic (MSA) – as well as some related molecules with intramolecular H-bonds (4-substituted picolinic acid *N*-oxides) were studied in an acetonitrile (ACN) solution. In order to evaluate the effect of proton positioning along the O–H...O bond on the measured chemical shifts the full geometry optimization was carried out, and <sup>17</sup>O magnetic shielding tensors were calculated using density functional theory (DFT). The modified hybrid functional PBE1PBE with the 6-311++G\*\* basis set and the gauge-including atomic orbital (GIAO) approach were applied. The solvent effect was taken into account by a polarized continuum model using the integral equation formalism (IEFPCM). Two stable structures were deduced for the PyO complexes with TCA and TFA that correspond to the H-bonds with and without proton transfer (PT). Two minima on the potential surface were separated by ca 0.2 Å. The experimental <sup>17</sup>O NMR spectra have shown that the PyO-TCA complex in ACN can be considered as H-bonding with incipient PT, whereas it is known from neutron diffraction that in its crystalline state PT occurs. The proton location in PyO-TFA due to the thermally induced proton sharing was found at the middle point. The <sup>17</sup>O NMR data for the acids with an intramolecular H-bond (nitroPANO, PANO and methoxyPANO) deviate from the general trend. The factors that can cause it, such as the substitution effect, persistence of nano-crystallites in a solution due to a low solubility, etc., have been discussed.

**Keywords:** NMR spectra, hydrogen bond, proton transfer, pyridine *N*-oxide

## 1. Introduction

Hydrogen bonding (H-bonding) is an important structural motif in a wide variety of molecular systems. It is still not completely understood and is constantly producing new surprises [1]. This particularly holds for the cases of very short H-bonds [2, 3]. The well-known effects are expressed there in a radically different manner relative to their analogs with moderate or long H-bond lengths.

The sensitivity of <sup>17</sup>O chemical shifts and nuclear quadrupole coupling constants to H-bonding has attracted attention for several decades [4–8]. Due to difficulties arising from the low

natural abundance of <sup>17</sup>O the investigations based on the <sup>17</sup>O properties have been gaining a wider publicity only recently [9–13]. However, investigations of examples with very short H-bonds are still rather scant [3, 4, 9, 14, 15]. On the other hand, such systems are of great interest to biochemical processes and material properties. Recent advances have shown that, with the availability of ultrahigh magnetic fields (e.g. 21 T), <sup>17</sup>O NMR becomes applicable in studies of biological macromolecules in both solution and solid states, see [16, 17] and references therein.

However, a systematic <sup>17</sup>O NMR investigation of the effects of a progressive proton displacement

from the proton donor to the acceptor, including the proton transfer influence on increasing H-bond strength, does not seem to be carried out yet. Such a gradual increase of bond strength resulting from changes in either the proton donating or accepting moieties can be achieved by appropriate substituting in the H-bonding partners whereby the groups forming the H-bond remain unchanged.

An appropriate series of gradually changing H-bonds can be formed by azine *N*-oxide complexes with acids. Moreover, compounds with corresponding intramolecular H-bonds lend themselves to comparative investigations of this type of bonding with the intermolecular ones that are in the same range of O...O distances. Azine *N*-oxide complexes with carboxylic acids have been fairly extensively investigated in the past [18–20]. These works were aimed mostly at demonstrating the relationships between the differences of pK's of the components and the spectroscopic evidence of the strength of the resulting H-bonds, such as the centre of gravity of the broad OH absorption in the FTIR spectra as well as <sup>1</sup>H and <sup>13</sup>C chemical shifts. The results were reviewed in Ref. [20].

Meanwhile, precise X-ray and neutron diffraction studies of representative *N*-oxide complexes with carboxylic acids and molecules with corresponding intramolecular H-bonds [21–24] have shown that the H-bonds are indeed extremely short, they are in the range between 2.41 and 2.44 Å, and that the protons may assume positions to either nearer acid oxygen or to *N*-oxygen, but in any case close to the middle of the O...O vector.

<sup>17</sup>O liquid-state NMR is a useful high-resolution technique to solve structural problems for small organic molecules. The fast reorientation of the molecules in solutions results in narrow spectral lines due to the averaging of quadrupolar interaction. Therefore, it appeared attractive to investigate H-bonding in a solution as reflected by <sup>17</sup>O chemical shifts. For this work we chose the complexes of pyridine *N*-oxide (PyO) with the following acids – acetic (AA), cyanoacetic (CyA), propionic (PA), trichloroacetic (TCA), trifluoroacetic (TFA), hydrochloric (HCl) and methanesulfonic (MSA) – as well as some related molecules with intramolecular H-bonds (derivatives of picolinic acid *N*-oxide, PANO) in acetonitrile solutions.

The acidity of the donor increases in the above order and thus the series of complexes covers the extreme cases without and with proton transfer. The predominant position of the proton was determined from the FTIR frequencies of protonation sensitive pyridine ring modes [25]. The <sup>13</sup>C chemical shifts of the ring carbon turned out to also be reliable indicators of the state of protonation [24, 26].

In addition to the experimental NMR work, DFT calculations have been done for the magnetic shielding tensor at a fairly high level of theory [26]. The calculations were carried out on complexes taking into account the solvent effect by a polarized continuum model using the integral equation formalism (IEFPCM).

## 2. Experiment

Acetonitrile (ACN), anhydrous, 99.8% from *Sigma-Aldrich*, was used as a solvent. In some cases, ACN was kept over the molecular sieves (3 Å) for several days. Commercial acids – acetic (AA), cyanoacetic (CyA), propionic (PA), trichloroacetic (TCA), trifluoroacetic (TFA), hydrochloric (HCl), methanesulfonic (MSA) and picolinic acid *N*-oxide (PANO) – were preliminary purified by standard methods. Water from TFA was removed by adding trifluoroacetic acid anhydride and subsequent distillation. The solutions of 1.0 M concentration in ACN were prepared by weighing ( $\pm 0.1$  mg) the components in a nitrogen filled dry box. Samples with PyO-HCl were prepared by direct dissolving of PyO-HCl crystals. The limited solubility in ACN allowed us to prepare the samples of 0.1 M concentration of PyO-HCl, 0.5 M for the PyO complex with MSA and ca. 0.3 M for PANO.

The 4-nitro derivative of PANO (nitroPANO) was synthesized in the Department of Organic Chemistry of Vilnius University by nitration of PANO using a slightly modified procedure than that reported in Ref. [27]. A mixture of 2-picolinic acid *N*-oxide (1 g, 6.36 mmol), conc. H<sub>2</sub>SO<sub>4</sub> (3 mL), and conc. HNO<sub>3</sub> (2.2 mL,  $d = 1.5$  g/cm<sup>3</sup>) was heated at 408 K under stirring for 3 h. After cooling to room temperature, the reaction mixture was poured to a crushed ice. The formed precipitate was filtered off, washed with water to pH = 7 and recrystallized from ethanol to give 0.4 g (31%)

of 4-nitropicolinic acid *N*-oxide, m. p. 422–423 K, Ref. [27]: m. p. 421 K. The 4-methoxy derivative of PANO (methoxyPANO) was synthesized in the National Institute of Chemistry (Ljubljana, Slovenia) by known procedures [27].

$^{17}\text{O}$  NMR experiments were carried out at room temperature ( $T = 298\text{ K}$ ) on a Bruker Avance III 400 WB NMR spectrometer operating at 400 and 54 MHz for  $^1\text{H}$  and  $^{17}\text{O}$ , respectively, using a BBO probe-head.  $\text{D}_2\text{O}$  in the capillary insert was used for reference in the  $^{17}\text{O}$  NMR spectra. In order to get a better signal-to-noise ratio the natural abundance  $^{17}\text{O}$  spectra were recorded using 10 mm tubes. The  $\pi/2$  pulses of  $22.5\ \mu\text{s}$  at the transmitter power of 70 W were applied using the acquisition time of 0.02 s and the recycle delay of 0.4 s. The number of scans was 400 000. The NMR spectra were processed using the Topsin 3.2 software. Additionally, the signal shapes and graphics were processed using the Microcal Origin package.

### 3. DFT calculations

Quantum chemical density functional theory calculations (DFT) were performed to gain the  $^{17}\text{O}$  NMR chemical shift information of the investigated molecular systems. After some testing, the hybrid gradient corrected functional of Perdew, Burke and Ernzerhof PBE1PBE [28], also known as PBE0, and the 6-311++G\*\* basis set [29] were adopted for full geometry optimizations and magnetic shielding tensor ( $\sigma$ ) calculations. Magnetic shielding tensor was calculated by using the gauge independent atomic orbital (GIAO) approach [30]. In the case of quantum chemical calculations for systems involving PyO, solvent effects were taken into account by a polarized continuum model using the integral equation formalism (IEFPCM) [31] along with the universal force field (UFF) atomic radii for the construction of the cavity as implemented in the Gaussian 03, Revision B.01 [32] suite of programs. In the case of quantum chemical calculations for systems involving PANO, solvent effects were modelled by the PCM [33] with the default settings as implemented in Gaussian 16, Revision A.03 [34].

The isotropic  $^{17}\text{O}$  NMR chemical shifts of the investigated molecules (H-complexes) were transformed to the  $\delta$ -scale using the Wasylshen proposed formula  $\delta = 307.9 - \sigma_{iso}$ , where  $\sigma_{iso}$

is the isotropic part of the calculated magnetic shielding tensor [35].

This approach was proven to be adequate in various cases earlier. For example, a fairly good agreement between the calculated and experimentally measured  $^1\text{H}$  and  $^{13}\text{C}$  NMR chemical shifts was obtained for the molecular systems involved in a strong H-bonding, but also for rather ‘inert’ species, e.g.  $-\text{CH}_3$  protons [24–26, 36, 37].

### 4. Results and discussion

Besides the H-bond systems studied experimentally, additional DFT calculations for the PyO complexes with water, tribromoacetic (TBA) and sulphuric ( $\text{H}_2\text{SO}_4$ ) acids were carried out for completeness. The complete series is presented in Fig. 1. The sequence of subjects was approximately ordered increasing the available values of acid dissociation constants (pKa) as well as the FTIR frequencies of PyO ring modes and the  $^{13}\text{C}$  chemical shifts of ring carbons [24–26]. It is clearly seen that the series splits into two parts – the neutral B...H–A bonds with  $r(\text{O–H})/R(\text{O...O}) < 0.5$  and the ionic pairs  $\text{BH}^+ \dots \text{A}^-$  with  $r(\text{O–H})/R(\text{O...O}) > 0.5$  that result from the proton transfer (PT). The PyO complexes with TCA and TFA occupy a special intriguing place in the series. Two stable structures were deduced for them by DFT calculation that correspond to the H-bond complexes with and without PT (Table 1). The PyO-TCA complex was noted by Hadži et al. as a peculiar system modelling the ‘proton kicking’ along the hydrogen bond [38].

The  $^{17}\text{O}$  chemical shifts were calculated after the full geometry optimization in ACN media. The calculated and experimental values are presented in Table 1. Some experimental  $^{17}\text{O}$  NMR spectra of the PyO and its complexes with acids are shown in Fig. 2.

Two signals appear in all  $^{17}\text{O}$  NMR spectra – one fairly sharp and the other rather broad signal (except for PyO-PA, in which only one signal appears). It is necessary to find out which of the observed signals belongs to *N*-oxide oxygen. This is easily accomplished by considering the  $^{17}\text{O}$  spectrum of a pyridine–carboxylic acid complex. Pyridine (Py) and its *N*-oxide have comparable proton accepting propensities in the solvents of a low polarity [39]. Therefore, the  $^{17}\text{O}$  chemical shifts of a carboxylic acid group should be similar with both acceptors,

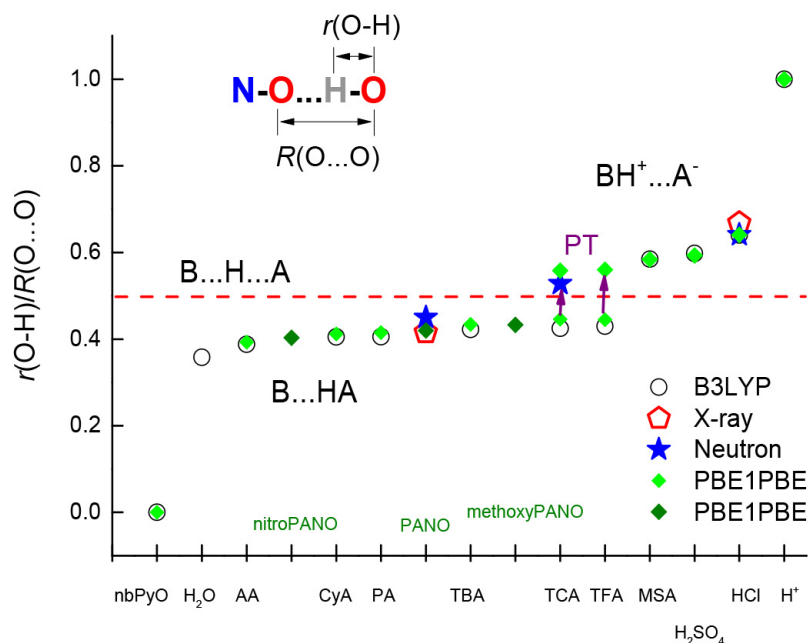


Fig. 1. The series of the studied H-bonded systems: the suspected proton transfer (PT) processes in PyO-TCA and PyO-TFA are shown by vertical arrows; the geometry of some complexes was optimized using the B3LYP functional for comparison; the experimental X-ray and neutron diffraction data were taken from Refs. [22–25].

Table 1. The optimized H-bond geometry and the  $^{17}\text{O}$  chemical shift values. The experimental values are relative to liquid  $\text{D}_2\text{O}$ ; the calculated values are in the Wasylishen scale, i.e.  $\delta = 307.9 \text{ ppm} - \sigma_{iso}$  [35].

Acid	$r(\text{O}-\text{H}), \text{\AA}$	$R(\text{O}\dots\text{O}), \text{\AA}$	$\delta(\text{COOH}), \text{ppm calc}$	$\delta(\text{N}-\text{O}), \text{ppm calc}$	$\delta(\text{N}-\text{O}), \text{ppm experiment}$	$\delta(\text{COOH}), \text{ppm experiment}$
Intermolecular H-bonds						
$\text{H}_2\text{O}$	0.982	2.744	–	314.07	–	–
AA	1.010	2.604	286.30	294.41	306	270
CyA	1.029	2.541	286.83	283.67	282	270
PA	1.030	2.540	295.65	283.41	278	278
TBA	1.052	2.492	278.19	271.63	–	–
TCA	1.056	2.486	275.65	267.79	276	265
TFA	1.064	2.476	279.91	265.88	240	262
TCA-PT	1.378	2.455	278.08	216.59	276	265
TFA-PT	1.384	2.459	284.47	215.23	240	262
MSA	1.463	2.501	–	204.43	210	–
$\text{H}_2\text{SO}_4$	1.518	2.541	–	197.7	–	–
HCl	1.844	2.881	–	214.05	220	–
Intramolecular H-bonds						
nitroPANO	1.001	2.4813	277.9	363.14	344	324
PANO	1.028	2.4441	278.1	299.76	193	271
methoxyPANO	1.047	2.418	283.0	260.92	170	246
Non-bonded PyO						
				339.74	345	

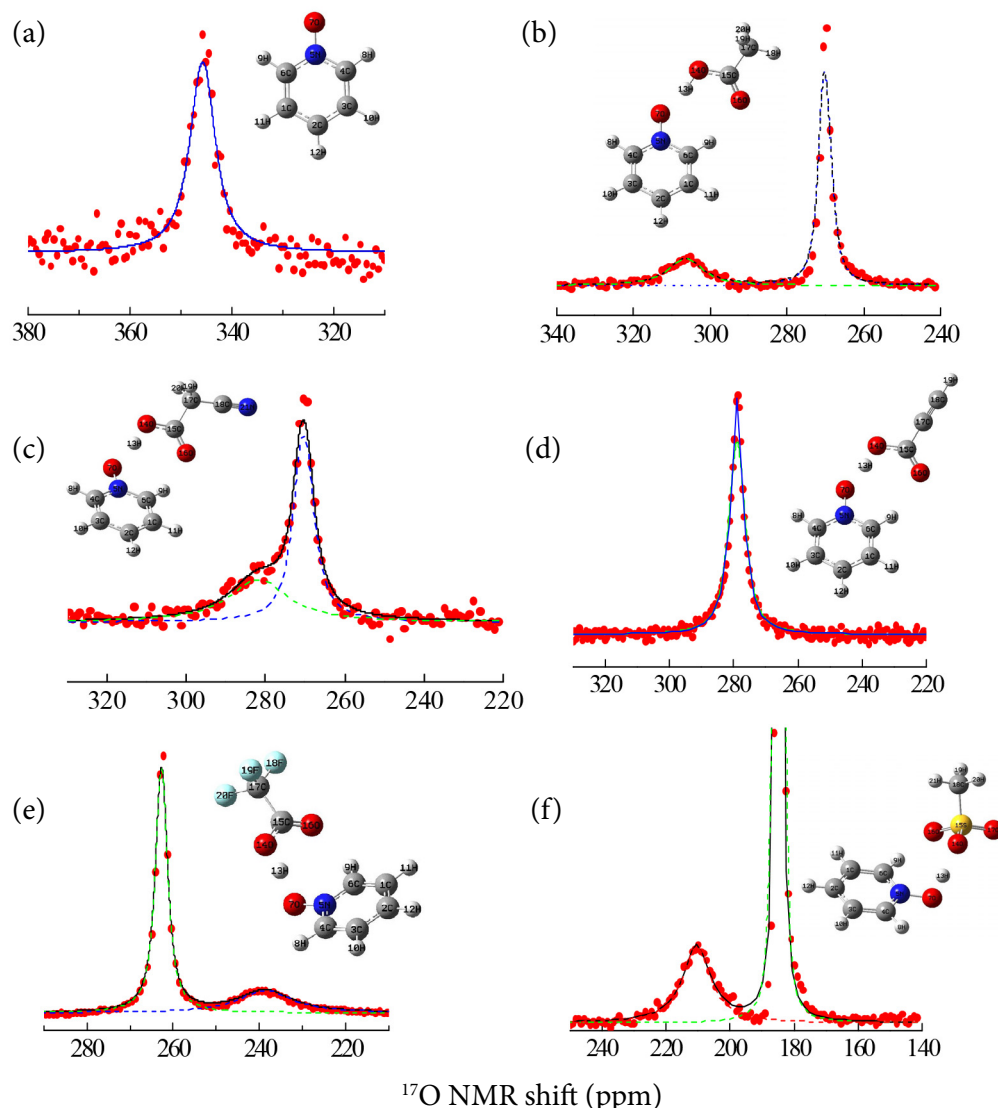


Fig. 2. The experimental  $^{17}\text{O}$  NMR spectra of PyO complexes in ACN solutions: (a) non-bonded PyO, (b) PyO-AA, (c) PyO-CyA, (d) PyO-PA, (e) PyO-TFA (all 1 M in ACN at 298 K) and (f) PyO-MSA (0.5 M in ACN at 343 K; the vertical scaling was chosen for a better presentation of the N-O signal, because of very different peak heights).  $\text{D}_2\text{O}$  in a capillary tube was used as a standard; the contours were approached by a Lorentzian shape using a nonlinear least-squares fitting.

while the *N*-oxide signal should not appear with the pyridine complex. Indeed, only one fairly narrow signal ( $\Delta\nu_{1/2} \approx 190 \pm 5$  Hz) was observed in the  $^{17}\text{O}$  NMR spectrum of Py-TFA at 269 ppm. The chemical shift is quite similar to one of the narrower signals in the spectrum of PyO-TFA at 262 ppm (Fig. 2(e), Table 1). Then the wider signal at  $\sim 240$  ppm belongs to *N*-oxide.

Next to be discussed is the reason for the appearance of a single  $^{17}\text{O}$  NMR signal of the carboxylic group instead of two. Two carboxylic sig-

nals would correspond to a unidentate bonding in the absence of averaging by a process that is fast on the NMR time scale. Static bidentate or dynamic averaging with a unidentate bonding will result in a single signal. Hence, one can conclude that in the studied cases the averaging process is fast on the NMR time scale.

The measured  $^{17}\text{O}$  chemical shifts of the carboxylic group cover the range between 262 and 278 ppm (Table 1). The experimental shift for nitroPANO drops to 324 ppm. This exceptional

case can be attributed to the  $\text{NO}_2$  substitution effect. The measured shifts are, roughly, between the shift of the hydroxylic oxygen (180 ppm) and one of the carbonyl oxygen (312 ppm) observed in the crystalline phthalic acid [9]. However, note that in benzoic acid only one  $^{17}\text{O}$  signal appears (270 ppm, [40]) both in the crystal and the solution.

From the limited experimental data concerning carboxylic acids and carboxylates in various environments and hydrogen bonding strengths it was concluded that the bond strength expressed in bond shortening increases magnetic shielding [41]. It is then somewhat surprising that the  $^{17}\text{O}$  magnetic shielding is the same in dimeric benzoic acid and potassium hydrogen dibenzoate despite the large difference in H-bond lengths (2.65 and 2.52 Å, respectively) [42]. However, these two examples differ in charge (one is neutral and the other anionic) and it is quite possible that competing influences are operating.

For COOH signals in the studied series, there is no obvious correlation between the  $^{17}\text{O}$  chemical shifts and progressive proton displacement from the acid to the accepting base oxygen as it is estimated from the calculated O–H and O...O distances (Fig. 3). This means that the  $^{17}\text{O}$  NMR signal of COOH is a bad spectral marker determining proton location.

Considering the N–O signal, there is a clear trend towards increasing the  $^{17}\text{O}$  magnetic shielding and thus decreasing  $^{17}\text{O}$  chemical shift

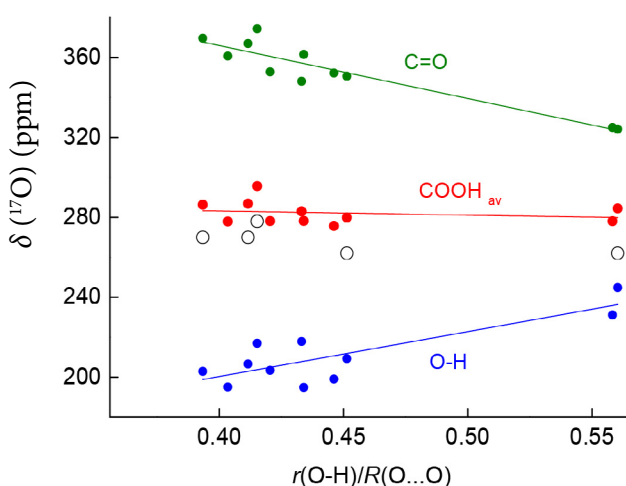


Fig. 3. The  $^{17}\text{O}$  chemical shifts of COOH signal in the studied series. The calculated and experimental chemical shift values are shown by filled and open circles, respectively.

with the increase of H-bond strength (Table 1). The observed increasing shielding corresponds to the previously noted effects of protic solvents on pyridine *N*-oxides [43, 44]. Notable is the parallel trend of the H-bonding and the substituent effects observed in the series of 4-substituted pyridine *N*-oxides [43, 45]. The result that  $\delta(\text{N-O})$  vs  $r(\text{O-H})/R(\text{O}\dots\text{O})$  was found being a continuous and almost linear function (Fig. 4) makes the N–O signal a proper spectral marker for the determination of proton location and thus for proton transfer.

There are several reasons that it can be even a better marker than the  $^1\text{H}$  NMR signal of the proton directly involved in the H-bonding.

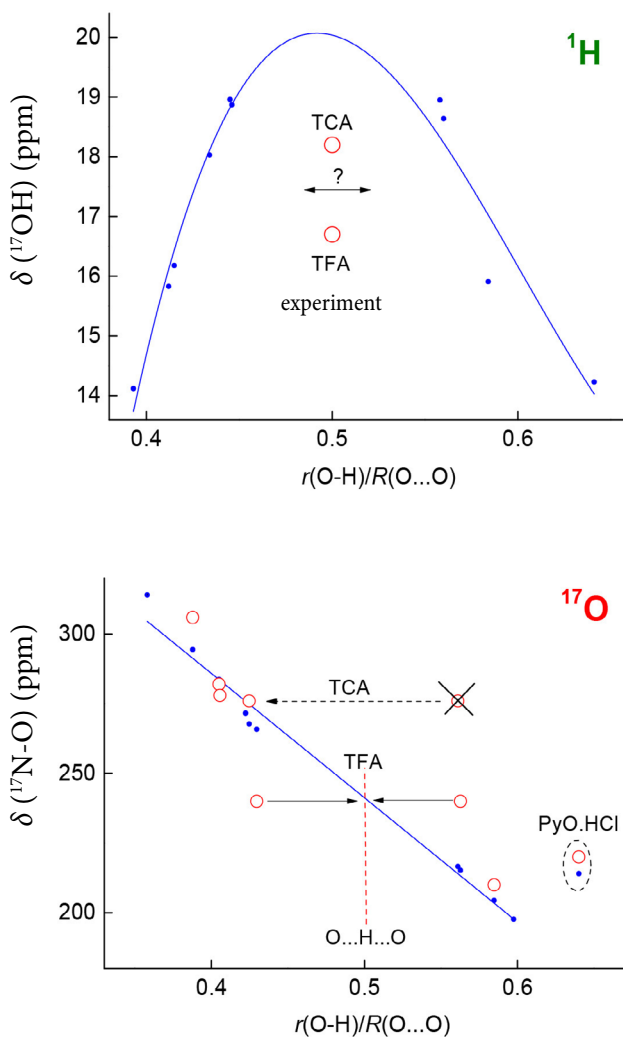


Fig. 4.  $^1\text{H}$  and  $^{17}\text{O}$  shifts in the complexes of PyO with acids (Table 1): • calculated points, ○ experiment. The drastic deviation of PyO-HCl from the linearity can be due to the different type of the H-bond ( $\text{OH}\dots\text{Cl}$ ). More comments in the text.

It is logical to suppose that the most sensitive to the geometry of H-bond should be the  $^1\text{H}$  chemical shift of the bridge proton,  $\delta(\text{OH})$ . However, its precise measurements often fail because of drying difficulties. In some systems, water molecules are very difficult to remove even applying molecular sieves, working in dry boxes or using other tricks (degassing, argon bubbling, etc.) [26, 46]. It is well-known that  $\delta(\text{OH})$  in strong H-bonds is high ( $\sim 14\text{--}20$  ppm) [20, 24, 26]. If the moisture is present, due to the dynamic averaging with the signal of water molecules ( $\sim 5$  ppm) the experimentally measured  $\delta(\text{OH})$  values can be shifted far up-field from the ‘true’ values. The lack of precision can influence the experimental data so seriously that the fine comparative evaluation of the H-bond state in the series is unsafe or even contradictory.

The next source of trouble is the shape of the function  $\delta(\text{OH}) = f(r(\text{O-H})/R(\text{O}\dots\text{O}))$ . It contains the up- and down-branches that correspond to the neutral  $\text{A-H}\dots\text{B}$  bonds and the ionic pairs  $\text{A}^-\dots\text{H}^+\text{B}$ , respectively, with the maximum at the middle point  $\text{A}\dots\text{H}\dots\text{B}$  (Fig. 4, also see [20, 26]). Therefore, sometimes it is puzzling to decide which of the two branches the experimentally measured  $\delta(\text{OH})$  should be attributed to. Such situation is shown in Fig. 4 for the PyO-TCA and PyO-TFA complexes, i.e. the most challenging subjects in the studied series.

The monotonous, i.e. with no extremum, dependence of the  $^{17}\text{O}$  chemical shift on  $r(\text{O-H})/R(\text{O}\dots\text{O})$  (Fig. 4) allows one to solve this problem unambiguously. It is clearly seen that the experimental point  $\delta(\text{N-O}) = 276$  ppm for PyO-TCA fits to the group of the points of neutral H-bonds. Among the PyO complexes with obviously weaker acids (AA, PA, CyA), it is the closest point to  $r(\text{O-H})/R(\text{O}\dots\text{O}) = 0.5$ , however, less than 0.5. Hence, the PyO-TCA complex in the ACN solution can be considered as H-bonding with incipient PT, whereas it is known from neutron diffraction data that in its crystalline state PT occurs [21].

In the case of PyO-TFA, the best fit of the experimental point  $\delta(\text{N-O}) = 240$  ppm brings it to  $r(\text{O-H})/R(\text{O}\dots\text{O}) = 0.5$ , i.e. to the location of a proton at the middle point. According to literature, this is a rare case and has to be discussed in more detail. A gape  $\Delta r(\text{O-H})/R(\text{O}\dots\text{O}) \approx 0.1$  is present around the centred position, i.e. the symmetric  $\text{O}\dots\text{H}\dots\text{O}$  bonding (Fig. 4). This indicates

that two minima on the potential surface that correspond to the complexes with and without PT are separated by ca  $0.2 \text{ \AA}$ . The thorough reviews of crystallographic data [47, 48] also point out that a certain gape should exist in the  $\text{O-H}$  vs  $\text{O}\dots\text{O}$  distances correlation for symmetric bonds. This is related with the two-site proton separation that was estimated as  $\sim 0.2 \text{ \AA}$  [48]. It was discussed that the change from the two-site proton to the centred proton occurs when the amplitude of thermal vibration along the H-bond reaches the top of the potential barrier. The direct experimental evidence of thermally induced proton migration was obtained for the H-bond complex of pentachlorophenol with 4-methylpyridine by neutron diffraction experiments carried out in the range of  $20\text{--}200 \text{ K}$  [49]. The proton gradually migrates with temperature, from being closer to the O atom (at high temperature) to being closer to the N atom (at low temperature). The middle point is passed through at  $\sim 90 \text{ K}$ . In the present work, the  $^{17}\text{O}$  NMR experiments were carried out at room temperature. This is sufficient to intensify the proton sharing between the donor and the acceptor in the PyO-TFA complex bringing the proton to the middle point.

The group of the acids with intramolecular H-bond (nitroPANO, PANO and methoxy-PANO) deviates from the general trend (Fig. 5). First of all, note a much steeper slope of  $\delta(\text{N-O})$  vs  $r(\text{O-H})/R(\text{O}\dots\text{O})$ . It is nice to see that this result of DFT calculations is confirmed by the experiment. The steeper slope can be explained to be due to the strong substituent effect that acts beside the H-bonding and PT. The overlap of both effects was deduced for 4-substituted PyOs and differentiated in the  $^{13}\text{C}$  NMR spectra [19]. However, the physical origin of significant discrepancies between the calculated and measured  $\delta(\text{N-O})$  values for the PANO group is not clear. There are several important factors that could cause it. The discrepancy could be related with a bad solubility of these acids in ACN ( $\sim 0.3 \text{ M}$  or even less). The outcome is that a part of material can persist as small (nano-sized?) crystallites that are mobile enough to contribute to the high resolution NMR signal. The solvent field effect modelled in the DFT calculations by PCM works improperly for such structures. As shown in [24] analyzing the solid-state  $^{13}\text{C}$  NMR spectra, the crystal force

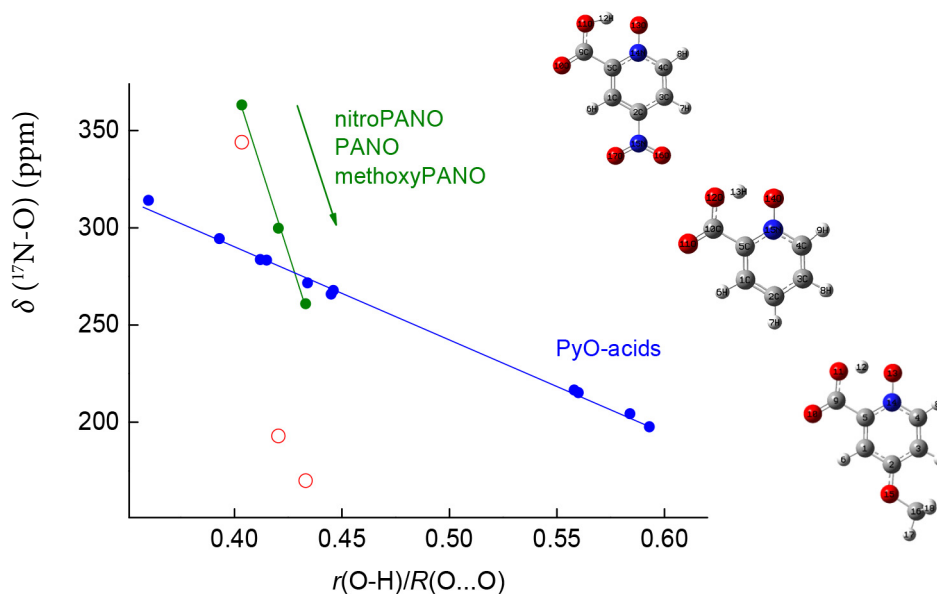


Fig. 5. The comparison of  $^{17}\text{O}$  chemical shifts of the N–O signal of 4-substituted picolinic acid *N*-oxides (PANO) and PyO-acid complexes. The calculated and experimental values are shown by filled and open circles, respectively.

field (CFF) in PANO forces the proton from donor to acceptor atoms much more strongly than the solvent reaction field (SRF).

The next factor can be related with the referencing of  $^{17}\text{O}$  chemical shifts. In the present work, the  $\delta$ -scale proposed by Wasylishen [35] was used. It can appear that this referencing is not the optimal one for the derivatives of PANO, and then it should be refined. The above questions were beyond the scope of the present paper and can be considered as a goal for future works.

## 5. Concluding remarks

The liquid-state  $^{17}\text{O}$  NMR spectra of pyridine *N*-oxide (PyO) complexes with the series of acids as well as some related molecules with intramolecular H-bonds (derivatives of picolinic acid *N*-oxide) were studied in the acetonitrile (ACN) solution. The N–O signal of proton acceptor was found to be a relevant spectral marker for the determination of proton location in the H-bond and proton transfer.

The full geometry optimization carried out using DFT has revealed that the studied series can be divided into two parts – the neutral B...H–A bonds for weaker acids and the ionic pairs  $\text{BH}^+\dots\text{A}^-$  for stronger acids. The PyO complexes with TCA and TFA occupy a challenging place. Two

stable structures were deduced for them that correspond to the H-bond complexes with and without PT. A gap  $\Delta r(\text{O–H})/R(\text{O}\dots\text{O}) \approx 0.1$  present around the symmetric  $\text{O}\dots\text{H}\dots\text{O}$  bonding means that two minima on the potential surface that correspond to the complexes with and without PT are separated by ca 0.2 Å.

The  $^{17}\text{O}$  NMR results have revealed that PyO in a solution forms with TCA the H-bond complex with incipient PT only, whereas it is known from neutron diffraction that in the crystalline state PT occurs. This can be considered as one more confirmation of the crucial influence of environment on the preferred proton location facilitating the PT process and that the crystal field forces the proton to move from the donor to acceptor atoms much stronger than the solvent reaction field.

The proton location in the PyO–TFA complex was found at the middle point. As the  $^{17}\text{O}$  NMR experiments were carried out at room temperature, this can be due to the thermally induced proton sharing. To our knowledge, this would be the first observation of the centred  $\text{O}\dots\text{H}\dots\text{O}$  bonding in liquid solutions.

It is likely that the discrepancy between the calculation and experimental  $^{17}\text{O}$  NMR data for PANO-series can be due to the persistence of nano-crystallites in the solution because of low solubility. The calculations of magnetic shielding using the cluster and periodic density functional theory with plane-wave



basis sets (DFT/PW) as well as Car–Parrinello molecular dynamics (CPMD) [22] would provide more information to elucidate this problem.

### Acknowledgements

In large part, the present work has been inspired by the ideas and suggestions of the pioneer of H-bonding research, Professor Dušan Hadži (1921–2019). We thank Professor Liudvikas Kimtys for his criticism and comments. The authors acknowledge the Center for Spectroscopic Characterization of Materials and Electronic/Molecular Processes ('Spectroversum', <http://www.spectroversum.ff.vu.lt>) for the use of spectroscopic equipment. Computations were performed on the resources at the high performance computing infrastructure of Vilnius University ('HPC Saulėtekis', <http://supercomputing.ff.vu.lt>).

### References

- [1] J. Stare, A. Gradišek, and J. Seliger, Nuclear quadrupole resonance supported by periodic quantum calculations: a sensitive tool for precise structural characterization of short hydrogen bonds, *Phys. Chem. Chem. Phys.* **22**, 27681–27689 (2020).
- [2] J. Stare, M. Hartl, L. Daemen, and J. Eckert, The very short hydrogen bond in the pyridine *N*-oxide – trichloroacetic acid complex: an inelastic neutron scattering and computational study, *Acta Chim. Slov.* **58**, 521–527 (2011).
- [3] J. Lu, I. Hung, A. Brinkmann, Z. Gan, X. Kong, and G. Wu, Solid-state  $^{17}\text{O}$  NMR reveals hydrogen-bonding energetics: not all low-barrier hydrogen bonds are strong, *Angew. Chem. Int. Ed.* **56**, 6166–6170 (2017).
- [4] I.J.F. Poplet and J.A.S. Smith,  $^{17}\text{O}$  and  $^2\text{H}$  quadrupole double resonance in some carboxylic acid dimers, *J. Chem. Soc. Faraday Trans. 2*, **77**, 1473–1485 (1981).
- [5] I.J.F. Poplet, M. Sabir, and J.A.S. Smith,  $^{17}\text{O}$  and  $^2\text{H}$  quadrupole double resonance in some acid carboxylates, *J. Chem. Soc. Faraday Trans. 2*, **77**, 1651–1668 (1981).
- [6] T.E.St. Amour, M.I. Burgar, B. Valentine, and D. Fiat,  $\text{O}^{17}$  NMR studies of substituent and hydrogen-bonding effects in substituted acetophenones and benzaldehydes, *J. Am. Chem. Soc.* **103**, 1128–1136 (1981).
- [7] L.G. Butler and T.L. Brown, Nuclear quadrupole coupling constants and hydrogen bonding. Molecular orbital study of oxygen-17 and deuterium field gradients in formaldehyde-water hydrogen bonding, *J. Am. Chem. Soc.* **103**, 6541–6549 (1981).
- [8] L.G. Butler, C.P. Cheng, and T.L. Brown, Oxygen-17 nuclear quadrupole double resonance. 6. Effects of hydrogen bonding, *J. Phys. Chem.* **85**, 2738–2740 (1981).
- [9] A.P. Howes, R. Jenkins, M.E. Smith, D.H.G. Crout, and R. Dupree, Influence of low-barrier hydrogen bonds on solid state  $^{17}\text{O}$  NMR spectra of labelled phthalate species, *Chem. Commun.* **16**, 1448–1449 (2001).
- [10] A. Wong, K.J. Pike, R. Jenkins, G.J. Clarkson, T. Anupold, A.P. Howes, D.H.G. Crout, A. Samoson, R. Dupree, and M.E. Smith, Experimental and theoretical  $^{17}\text{O}$  NMR study of the hydrogen-bonding on C=O and O–H oxygens in carboxylic solids, *J. Phys. Chem. A* **110**, 1824–1835 (2006).
- [11] K.J. Pike, V. Lemaître, A. Kukol, T. Anupold, A. Samoson, A.P. Howes, A. Watts, M.E. Smith, and R. Dupree, Solid-State  $^{17}\text{O}$  NMR of amino acids, *J. Phys. Chem. B* **108**, 9256–9263 (2004).
- [12] V. Lemaître, M.E. Smith, and A. Watts, A review of oxygen-17 solid-state NMR of organic materials – towards biological applications, *Solid State Nucl. Magn. Reson.* **26**, 215–235 (2004).
- [13] J.D. Bazak, A.R. Wong, K. Duanmu, K.S. Han, D. Reed, and V. Murugesan, Concentration-dependent solvation structure and dynamics of aqueous sulfuric acid using multinuclear NMR and DFT, *J. Phys. Chem. B* **125**, 5089–5099 (2021).
- [14] P. Rubini, D. Champmartin, and X. Assfeld, Determination of the  $^{17}\text{O}$  quadrupolar coupling constant and the  $^{13}\text{C}$  shielding tensor anisotropy in solution for molecules containing a COOH group. NMR relaxation study and theoretical calculations, *J. Chim. Phys.* **95**, 366–376 (1998).
- [15] J.E. Gready, G.B. Bacskey, and N.S. Hush, Comparison of the effects of symmetric versus

- asymmetric H-bonding on  $^2\text{H}$  and  $^{17}\text{O}$  nuclear quadrupole coupling constants: application to formic acid and the hydrogen diformate anion, *Chem. Phys.* **64**, 1–17 (1982).
- [16] G. Wu, Solid-state  $^{17}\text{O}$  NMR studies of organic and biological molecules: recent advances and future directions, *Solid State Nucl. Magn. Reson.* **73**, 1–14 (2016).
- [17] A.W. Tang, X. Kong, V. Terskikh, and G. Wu, Solid-state  $^{17}\text{O}$  NMR of unstable acyl-enzyme intermediates: a direct probe of hydrogen bonding interactions in the oxyanion hole of serine proteases, *J. Phys. Chem. B* **120**, 11142–11150 (2016).
- [18] Z. Dega-Szafran, M. Grunwald-Wypianska, and M. Szafran, Evidence for a single minimum potential for hydrogen bonds of pyridine *N*-oxide complexes with dichloroacetic acid in dichloromethane, *Spectrochim. Acta A* **47**, 125–131 (1991).
- [19] M. Szafran, B. Brycki, Z. Dega-Szafran, and B. Nowak-Wydra, Differentiation of substituent effects from hydrogen bonding and protonation effects in carbon-13 NMR spectra of pyridine *N*-oxide, *J. Chem. Soc. Perkin Trans. 2*, 1161–1166 (1991).
- [20] M. Szafran, Recent aspects of the proton transfer reaction in H-bonded complexes, *J. Mol. Struct.* **381**, 39–64 (1996).
- [21] K.D. Eichhorn, Neutron structure analysis of 1-hydroxy pyridinium trichloroacetate,  $\text{C}_7\text{H}_6\text{Cl}_3\text{NO}_3$ , at 120 K, *Z. Kristallographie* **195**, 205–220 (1991).
- [22] J. Panek, J. Stare, and D. Hadži, From the isolated molecule to oligomers and the crystal: A static density functional theory and Car-Parrinello molecular dynamics study of geometry and potential function modifications of the short intramolecular hydrogen bond in picolinic acid *N*-oxide, *J. Phys. Chem. A* **108**, 7417–7423 (2004).
- [23] T. Steiner, A.M.M. Schreurs, M. Lutz, and J. Kroon, Strong intramolecular O–H...O hydrogen bonds in quinaldic acid *N*-oxide and picolinic acid *N*-oxide, *Acta Crystallogr. Sect. C* **56**, 577–579 (2000).
- [24] V. Balevičius, A. Maršalka, V. Klimavičius, L. Dągys, M. Gdaniec, I. Svoboda, and H. Fuess, NMR and XRD study of hydrogen bonding in picolinic acid *N*-oxide in crystalline state and solutions: media and temperature effects on potential energy surface, *J. Phys. Chem. A* **122**, 6894–6902 (2018).
- [25] V. Balevičius, K. Aidas, I. Svoboda, and H. Fuess, Hydrogen bonding in pyridine *N*-oxide/acid systems: proton transfer and fine details revealed by FTIR, NMR, and X-ray diffraction, *J. Phys. Chem. A* **116**, 8753–8761 (2012).
- [26] V. Balevičius, Z. Gdaniec, and K. Aidas, NMR and DFT study on media effects on proton transfer in hydrogen bonding: concept of molecular probe with an application to ionic and super-polar liquids, *Phys. Chem. Chem. Phys.* **11**, 8592–8600 (2009).
- [27] E. von Profft and W. Steinke, *N*-Oxyde substituerter Picolinsäuren, *J. Prakt. Chem.* **13**, 58–75 (1961).
- [28] C. Adamo and V. Barone, Toward reliable density functional methods without adjustable parameters: The PBE0 model, *J. Chem. Phys.* **110**, 6158–6169 (1999).
- [29] R. Krishnan, J.S. Binkley, R. Seeger, and J.A. Pople, Self-consistent molecular orbital methods. XX. A basis set for correlated wave functions, *J. Chem. Phys.* **72**, 650–654 (1980).
- [30] K. Wolinski, J.F. Hilton, and P. Pulay, Efficient implementation of the gauge-independent atomic orbital method for NMR chemical shift calculations, *J. Am. Chem. Soc.* **112**, 8251–8260 (1990).
- [31] J. Tomasi, B. Mennucci, and R. Cammi, Quantum mechanical continuum solvation models, *Chem. Rev.* **105**, 2999–3094 (2005).
- [32] M.J. Frisch, G.W. Trucks, H.B. Schlegel, G.E. Scuseria, M.A. Robb, J.R. Cheeseman, J.A. Montgomery Jr., T. Vreven, K.N. Kudin, J.C. Burant, et al., *Gaussian 03, Revision B.01* (Gaussian, Inc., Pittsburgh PA, 2003).
- [33] G. Scalmani and M.J. Frisch, Continuous surface charge polarizable continuum models of solvation. I. General formalism, *J. Chem. Phys.* **132**, 114110 (2010).

- [34] M.J. Frisch, G.W. Trucks, H.B. Schlegel, G.E. Scuseria, M.A. Robb, J.R. Cheeseman, G. Scalmani, V. Barone, G.A. Petersson, H. Nakatsuji, et al., *Gaussian 16, Revision A.03* (Gaussian, Inc., Wallingford CT, 2016).
- [35] R.E. Wasylishen, S. Mooibroek, and B. Macdonald, A more reliable oxygen-17 absolute chemical shielding scale, *J. Chem. Phys.* **81**, 1057 (1984).
- [36] K. Aidas, A. Maršalka, Z. Gdaniec, and V. Balevičius, A  $^{13}\text{C}$  NMR and density functional theory study of critical behaviour of binary water/2,6-lutidine solution, *Lith. J. Phys.* **47**, 443–449 (2007).
- [37] K. Aidas and V. Balevičius, Proton transfer in H-bond: possibility of short-range order solvent effect, *J. Mol. Liquids* **127**, 134–138 (2006).
- [38] J. Stare, F. Merzel, and D. Hadži, in: *New Methods in Molecular Spectroscopy* (Wrocław University, 2002) p. 28.
- [39] M.H. Abraham, P.P. Duce, P.L. Grellier, D.V. Prior, J.J. Morris, and P.J. Taylor, Hydrogen-bonding. Part 5. A thermodynamically-based scale of solute hydrogen-bond acidity, *Tetrahedron Lett.* **29**, 1578–1590 (1988).
- [40] D. Monti, F. Orsini, and G.S. Ricca, Oxygen-17 NMR spectroscopy: effects of substituents on chemical shifts for  $\sigma\text{-m-p}^-$  substituted benzoic acids, phenylacetic and methyl benzoates, *Spectrosc. Lett.* **19**, 91–99 (1986).
- [41] S. Kuroki, S. Ando, and I. Ando, An MO study of nuclear quadrupolar coupling constant and nuclear shielding of the carbonyl oxygen in solid peptides with hydrogen bonds, *Chem. Phys.* **195**, 107–116 (1995).
- [42] S. Dong, K. Yamada, and G. Wu, Oxygen-17 nuclear magnetic resonance of organic solids, *Z. Naturforsch. A* **55**, 21–28 (2000).
- [43] D.W. Boykin, A.L. Baumstark, and P. Balakrishnan,  $^{17}\text{O}$  NMR spectroscopy of 4-substituted pyridine *N*-oxides: substituent and solvent effects, *Magn. Reson. Chem.* **23**, 276–279 (1985).
- [44] D.W. Boykin, P. Balakrishnan, and A.L. Baumstark, Natural abundance  $^{17}\text{O}$  NMR spectroscopy of heterocyclic *N*-oxides and di *N*-oxides. Structural effects, *J. Heterocycl. Chem.* **22**, 981–984 (1985).
- [45] P.M. Woyciesjes, N. Janes, S. Ganapathy, Y. Hiyaama, T.L. Brown, and E. Oldfield, Nitrogen and oxygen nuclear quadrupole and nuclear magnetic resonance spectroscopic study of N–O bonding in pyridine 1-oxides, *Magn. Reson. Chem.* **23**, 315–321 (1985).
- [46] A. Maršalka, L. Dagys, V. Jakubkienė, S. Tumkevičius, and V. Balevičius,  $^1\text{H}$  and  $^{17}\text{O}$  NMR study of H-bond dynamics in picolinic acid *N*-oxide solutions in acetonitrile- $h_3$  and acetonitrile- $d_3$ : novel aspects of old casus, *Chem. Phys.* **513**, 17–22 (2018).
- [47] M. Ichikawa, Hydrogen-bond geometry and its isotope effect in crystals with OHO bonds – revisited, *J. Mol. Struct.* **552**, 63–70 (2000).
- [48] R.J. Nelmes, Structural studies of KDP and the KDP-type transition by neutron and x-ray diffraction: 1970–1985, *Ferroelectrics* **71**, 87–123 (1987).
- [49] T. Steiner, I. Majerz, and C.C. Wilson, First O–H–N hydrogen bond with a centered proton obtained by thermally induced proton migration, *Angew. Chem. Int. Ed.* **40**, 2651–2654 (2001).

## VANDENILINIO RYŠIO TYRIMAS TAIKANT $^{17}\text{O}$ BMR IR TANKIO FUNKCIONALO TEORIJĄ: PROTONO DALYBOS IR PRADINĖ PERNAŠA

V. Balevičius<sup>a</sup>, K. Aidas<sup>a</sup>, A. Maršalka<sup>a</sup>, F. Kuliešius<sup>a</sup>, V. Jakubkienė<sup>b</sup>, S. Tumkevičius<sup>b</sup>

<sup>a</sup> *Vilniaus universiteto Cheminės fizikos institutas, Vilnius, Lietuva*

<sup>b</sup> *Vilniaus universiteto Organinės chemijos katedra, Vilnius, Lietuva*

### Santrauka

Šiame darbe buvo eksperimentiškai ištirti piridino *N*-oksido vandenilinio ryšio (H-ryšio) kompleksų su rūgštimis (acto (AA), cianacto (CyA), propiolo (PA), vandenilio chloridu (HCl), metansulfonrūgštimi (MSA)) bei kai kurių panašių molekulių su vidiniais H-ryšiais (4-pakeisti pikolino rūgšties *N*-oksidai)  $^{17}\text{O}$  BMR spektrai acetonitrilo (ACN) tirpaluose. Siekiant nustatyti protono lokalizaciją ir H-ryšių geometriją bei terpės reakcijos lauko įtaką išmatuotiesiems  $^{17}\text{O}$  cheminiams poslinkiams, pasitelkus kvantinės mechanikos tankio funkcionalo teoriją (DFT), buvo visiškai optimizuota H-ryšio kompleksų geometrija ir apskaičiuoti deguonies magnetinio ekranavimo tenzoriai. Skaičiavimai atlikti taikant modifikuotą hibridinį Perdew, Burke ir Ernzerhof funkcionalą (PBE1PBE) kartu su 6-311++G\*\* bazinių funkcijų rinkiniu bei GIAO atominių orbitalių artinį. Dielektrinės terpės (ACN) reakcijos laukas buvo įskaitytas pritaikant poliarizuojamojo kontinuumo modelį ir naudojant integralinių lygčių

formalizmą (IEFPCM). PyO kompleksams su TCA ir TFA buvo nustatyta po dvi energetiškai stabilias struktūras, kurios priklauso H-ryšiams su protono pernaša (PP) ir be jos. Atstumas, skiriantis šių struktūrų potencialinės energijos duobes, yra apie 0,2 Å. Eksperimentiškai išmatuoti  $^{17}\text{O}$  BMR spektrai leidžia teigti, kad ACN tirpale PyO-TCA kompleksas gali būti apibūdintas kaip H-ryšys su pradine PP. Tai esmingai skiriasi nuo jų H-ryšio kristale, kur iš neutronų difrakcijos duomenų galima matyti, kad PP vyksta. PyO-TFA komplekse dėl termiškai sukeltų protono dalybų protonas yra lokalizuotas ties H-ryšio centru (O...H...O).  $^{17}\text{O}$  BMR duomenys, gautieji molekulėms su vidiniais H-ryšiais (4-pakeisti pikolino rūgšties *N*-oksidai), skiriasi nuo bendrosios schemos, nustatytos PyO-rūgšties kompleksams. Darbe aptartos galimos to priežastys, tarp kurių – cheminių pakaitų ir H-ryšio efektų persiklojimas, tirpinamųjų medžiagų nanokristalitai, kurie išlieka tirpale dėl blogo tirpumo ir kt.